Monthly Notices
of the
ROYAL ASTRONOMICAL SOCIETY

MNRAS **527,** 10604–10614 (2024)
Advance Access publication 2023 December 18

https://doi.org/10.1093/mnras/stad3854

Experimental H_2O formation on carbonaceous dust grains at temperatures up to 85 K

F. Grieco [1,2]★ F. Dulieu,[1] I. De Looze[2] and S. Baouche[1]

[1]*CY Cergy Paris Université, Observatoire de Paris, PSL University, Sorbonne Université, CNRS, LERMA, F-95000 Cergy, France*
[2]*University of Ghent, Department of Physics and Astronomy, Ghent, Belgium*

Accepted 2023 December 12. Received 2023 December 11; in original form 2023 October 4

ABSTRACT

Water represents the main component of the icy mantles on dust grains, it is of extreme importance for the formation of new species and it represents the main component for life. Water is observed both in the gas-phase and frozen in the interstellar medium (ISM), where the solid-phase formation route has been proven essential to explain abundances in molecular clouds. So far, experiments have focused on very low temperatures (around 10 K). We present the experimental evidence of solid water formation on coronene, PAH-like surface, for a higher range of temperatures. Water is efficiently formed up to 85 K through the interaction of oxygen and hydrogen atomic beams with a carbonaceous grain analogue. The beams are aimed towards the surface connected to a cryostat exploring temperatures from 10 to 100 K. The results are obtained with a QMS and analysed through a temperature-programmed desorption technique. We observe an efficient water formation on coronene from 10 up to 85 K mimicking the temperature conditions from the dense ISM to translucent regions, where the ice mantle onset is supposed to start. The results show the catalytic nature of coronene and the role of chemisorption processes. The formation of the icy mantles could be happening in less dense and warmer environments, helping explaining oxygen depletion in the ISM. The findings have several applications such as the disappearance of PAHs in translucent regions and the snowlines of protoplanetary discs. We stress on how *JWST* projects characterizing PAHs can be combined with H_2O observations to study water formation at warm temperatures.

Key words: astrochemistry – methods: laboratory: atomic – ISM: atoms – ISM: clouds – dust, extinction – ISM: molecules.

1 INTRODUCTION

1.1 Experiments and theoretical studies on water formation routes

The study of water formation in the interstellar medium (ISM) is very important as the main molecule constituting icy mantles, storing, and catalysing the formation of potential biologically relevant structures. Water is observed as vapour in the gas-phase in cold regions with temperatures below 50 K, such as molecular clouds (Caselli et al. 2010), but also frozen, up to about 2×10^{-4} in abundance, with respect to H_2, in colder objects. The frozen water is believed to consist mostly of icy mantles on dust grains (Boogert, Gerakines & Whittet 2015). In both the solid and gas phases, water is considered to lock most of the elemental oxygen into the molecular form (van Dishoeck, Herbst & Neufeld 2013). Also, interstellar water has a very strong implication in planets' habitability research. Apart from its important role as a major factor for life, it can give indications on eventually detectable biospheres. Having more details about the abundance of solid water, its freezing and melting temperatures can help constraining the so-called habitability index (Silva et al. 2017). Understanding the origins of water is also key in several other fields and there are still many questions regarding when and where ices are formed in both planet-forming discs and stellar systems, for example. They are thought to possibly form through two main processes: (i) in the dense ISM, ices could form in cold molecular cloud cores prior to star formation. Here, interstellar ices would be incorporated into all planet-forming discs. (ii) They could also be products of reprocessing within the central star nebula. In this case, we would have large water abundance variations for different stellar systems (Cleeves et al. 2014). The link between the formation and the observation of water on planetary systems remains of fundamental importance in astrochemistry. The study of its chemical and physical evolution can therefore give more info about the origin of water in Solar system bodies (Jensen et al. 2019). For example terrestrial and sub-Neptune planets should be forming water in the inner regions of protoplanetary discs where water plays a crucial role. Besides eventually needing a water reservoir for their formation, this rises the question about the birthplace of the available water, if *in situ* or from the outer disc. Understanding the position of the snowline as well as the role of dust/ices and temperatures are interesting points since the replenishment of both gas and dust from the outer disc could be one of the main water reservoir contributors (Perotti et al. 2023). Finally, the icy mantle-covered dust grains in the rotating discs around stars come from the accretion of gas on to dust in molecular clouds, from where the planets will be afterwards formed (van Dishoeck 2004). Assessing how the ice mantles form,

★ E-mail: francesco.grieco@ugent.be

in which regions and under which physical conditions and range of temperatures could therefore be linked to many other aspects at bigger scales. However, independently from specific applications, studying water formation requires an understanding of how water interacts with a dust grain surface, how the latter contributes to its formation and which ranges of temperatures are involved in those processes. In the last decades, there have been different laboratory studies and models trying to unveil the water formation routes on dust grains, focusing on three main possible chemical routes initiated with different reaction (Tielens & Hagen 1982): (1) O+H reactions (Dulieu et al. 2010; Vidali, Jing & He 2013); 2) hydrogenation of O_2 (Ioppolo et al. 2008; Matar et al. 2008, Oba et al. 2009); and (3) hydrogenation of O_3 (Mokrane et al. 2009; Romanzin et al. 2011).

All the models and experiments that have helped us understanding water formation processes are often carried out in different conditions. This makes it challenging to directly apply and interpret those findings for several ISM regions. Thus, there are still many open questions that need to be answered in this field. Nevertheless, it is now clear that the formation of water molecules in the gas-phase is incapable of explaining the observed abundances in molecular clouds, especially for the solid form (Parise, Ceccarelli & Maret 2005, Ceccarelli et al. 2007). In general, water molecules are mainly believed to be synthesized by atomic reactions involving H and O atoms on pre-existing silicate or carbonaceous grains at around 10 K. However, OH+H_2 may probably be another important alternative, as explained by the difference in deuteration efficiency for the D and HD routes (Kristensen et al. 2011; Oba et al. 2012).

The first formation route (O+H reactions) has been studied intensively by Cuppen & Herbst (2007) who found it to be the main one for O atoms on grains in cool diffuse clouds with no activation barrier (in the gas-phase), where H and O atoms are the major gas-phase species: $O + H \rightarrow OH$ (reaction 1); $OH + H \rightarrow H_2O$.

From reaction 1, OH can also follow a different path, encountering molecular hydrogen already adsorbed on the grain, as shown below (activation energy of 5.16 kcal mol^{-1} in the gas-phase (McCormac 1973)): $OH + H_2 \rightarrow H_2O + H$.

The second route relates to the hydrogenation of O_2. Tielens & Hagen (1982) proposed: $O + O \rightarrow O_2$;

$O_2 + H \rightarrow HO_2$ (no barrier); $HO_2 + H \rightarrow H_2O_2$;
$H_2O_2 + H \rightarrow H_2O + OH$.

Those are the main routes in cold molecular clouds where H_2 molecules are the major gas-phase species. There are laboratory experiments studying this second water formation network reporting the formation of water molecules under conditions mimicking cold interstellar molecular clouds. By starting from reactions of cold H atoms with solid O_2 molecules at 10 K, they found the following reaction steps to be the most efficient:

$O_2 + 2H \rightarrow H_2O_2$; $H_2O_2 + H \rightarrow H_2O + OH$; (Miyauchi et al. 2008; Kristensen et al. 2011).

For the third route, since the chemical models by Tielens & Hagen (1982), there have been many others confirming the hydrogenation of O_3 leading to water formation on grains. Parise (2004) proposed a water formation scheme where O_3 molecules react with H or D atoms to form OH or OD, and subsequently the reaction H_2+OH/OD would lead to H_2O/HDO. This has been confirmed experimentally by Oba et al. (2012). The Monte Carlo simulations of Cuppen & Herbst (2007) emphasize the non-negligible contribution from the H+H_2O_2 reaction (H_2O_2 being a product of the H+O_2 pathway) and the unusual high abundance of reactants such as OH and O_3.

It is also relevant to mention experiments on water formation via OH radicals. Oba et al. (2011) produced them in a H_2O microwave-discharge plasma, where water was formed at 40 and 50 K, but not at 60 K, together with H_2O_2. The study shows the importance of OH radicals as well as the possibility to investigate water formation at higher dust grain temperatures and the role of the surface. Lastly, there have been several experimental studies reporting water formation on dust grains or in astrophysically relevant conditions. The reality is that, under dark cloud conditions, only the very first monolayer grows on bare silicate or carbonaceous grains (Papoular 2005), most water molecules should be subsequently synthesized on a surface mainly composed of ices. Dulieu et al. (2010) ran an investigation on how water formation continues on the icy surfaces of cosmic grains. At 10 K, deuterated water molecules were formed with a high efficiency (about 50 per cent) by exposing amorphous water ice substrate to O and D atoms. Furthermore, the details about all the possible different networks have been deeply investigated by Kristensen et al. (2011). Later on, it has been also shown that, if water forms in excess of energy, the newly formed molecules can undergo chemical desorption mechanisms. This process is more efficient for harder surfaces (Dulieu et al. 2014). Until now, all the studies have only considered water formation through physisorption mechanisms. However, we have already demonstrated the importance of chemisorption processes for H_2 formation on carbonaceous dust grains at temperatures up to 250 K (Grieco et al. 2023). Therefore we want to keep investigating the role of those surfaces for the formation of small and important molecules in the ISM, such as H_2O in this paper. Reporting the main H_2O formation pathways and the state-of-the-art of several studies on dust grains gives us the right context to address the main goal of this work: the experimental study of H_2O through its formation and interaction with a carbonaceous surface for a higher range of temperatures. An overview of different studies of PAHs and ice interactions are given in the following section.

1.2 PAHs in ISM, O, and H atoms interactions and interstellar ices

Already in the 1970s, broad midinfrared (mid-IR) emission features present in almost all objects (bright H II regions, surfaces of dark clouds, and the general ISM) were attributed to polycyclic aromatic hydrocarbon (PAH), molecules of about 50 carbon atoms (Allamandola, Tielens & Barker 1989; Puget & Leger 1989).

PAHs are ubiquitous [10^{-7} n(H)$^{-1}$] in the ISM. These species play an important role in the heating of neutral gas, in the ionization balance in molecular clouds as well as in the phase structure of the ISM and its ion-molecule chemistry. Since then, models have provided much insight into the formation and evolution of interstellar PAHs. PAHs represent an important reservoir of interstellar elemental carbon (fc of about 3.5×10^{-2}) and they can be found in both gas and solid phases in the ISM (Salama 2008; Tielens 2008). They are supposed to either form in the envelopes around carbon stars by a series of reactions building up large PAHs from small carbon chains, or by top-down routes through fragmentation of large grains in the ISM (Chastenet et al. 2019). The main part of the PAH population is bigger than C_{40} (Jochims, Baumgärtel & Leach 1999) and PAHs smaller than this will be destroyed by ultraviolet (UV) irradiation in regions of high photon flux, coagulate in dense regions or they can survive in icy grain mantles in molecular clouds. Also, many new small cyclic *N*-bearing carbon molecules have been detected in the molecular cloud TMC-1. McGuire et al. (2021) analyse and discuss *in situ* gas-phase formation from smaller organic molecules, but they are not able to explain and match the observed abundances with neither top-down or bottom-up pathways. The formation of those molecules in molecular clouds and their

survival in those conditions in order to be observed could be an indication of the strong stabilization that small aromatic structures can provide. This opens the doors to other possible formation routes that should be considered for those heteroatoms-bearing structures, as e.g. chemisorption processes involving C and N atoms from the gas-phase landing on the surface and further form new functional groups on the ring.

In the present experimental study, the PAH used as interacting surface is coronene, a molecule of 24 carbon atoms ($C_{24}H_{12}$). Coronene is often used in the laboratory to model more interstellar-relevant PAHs. In fact, it is often considered as an archetypal interstellar PAH. It is believed to represent a favoured structure during PAH growth and formation (Oomens et al. 2001). $C_{24}H_{12}$ is indeed one of the largest PAHs that can be easily manipulated in the laboratory and using this type of surfaces is a standard experimental approach. Coronene is also found to be relatively resistant to UV photodecomposition (Noble et al. 2017). During their lifetime in the ISM, PAHs can be both functionalized with chemical side groups, or be substituted with heteroatoms (observations: Peeters et al. 2002; calculations: Sadjadi, Zhang & Kwok 2015; experiments: Bernstein et al. 1999; Bouwman et al. 2011; Guennoun, Aupetit & Mascetti 2011; Gudipati & Yang 2012; Cook et al. 2015; Noble et al. 2020).

In cold regions of the ISM, PAHs are expected to be frozen out on dust grains. There are laboratory experiments investigating water–ice and PAH mixtures and they show that superhydrogenated PAHs are produced together with PAHs with alcohol and ketone functional groups. These studies suggest that oxygen-bearing PAH species could be formed in the ISM on icy grains (Jaganathan et al. 2022). In fact, laboratory studies on the reactivity of PAHs and water molecules show an efficient formation of oxygenated PAHs, higher than the actual abundance observed in denser regions. Destruction routes of such species should therefore be efficient (Thrower et al. 2014; Noble et al. 2017). Specifically, in regions with higher extinction (A_V higher than 2) it is not clear whether PAHs exist and under what form. PAHs can condense on small grains or be incorporated in icy mantles. Indeed A_V around two correspond to the onset of detection of solid water ice in the ISM (Boogert, Gerakines & Whittet 2015). In these edge zones, PAHs in water ice can become oxygenated or be chemically transformed in the gas-phase. O atoms are responsible for these changes. In particular they can be the main actors since they can remain in the gas-phase or they are kept in the form of water. Actually, O atoms can easily be inserted on the edges of small PAHs, and thus coronene, but they can also push the chemical destruction of these molecules into smaller ones, such as ketene, and enhance their entrance in the ISM (Dulieu et al. 2019). Finally, another important point is the role of dust grains as catalysts, and specifically PAHs, for the formation and thus abundance of molecules in the cold ISM, such as H_2, H_2O, H_2CO, and CH_3OH, that cannot be synthesized solely by gas-phase reactions. One of the simplest water formation routes ever proposed is the sequential hydrogenation of O atoms, producing OH and then water, as shown experimentally (Dulieu et al. 2010). The interaction of the incoming species (H, OH, and CO) with PAHs has been recently modelled. They can react with axial H atoms of hydrogenated PAHs following the Eley–Rideal mechanism and H_2O is produced with no activation barrier (Ferullo, Zubieta & Belelli 2019). As introduced in the previous section, there are several water formation routes involving dust grains. The study of the role of PAHs on icy mantles, their reactivity with water, the interaction with H and O atoms to eventually form water is therefore of fundamental importance in this field. In our laboratory, we studied the behaviour of hydrogen and oxygen atoms sent on to coronene and the eventual formation of water on the surface at several temperatures up to 85 K. This work has the aim of verifying if the main H_2O routes, when a typical PAH-like surface is used, can compete with the incorporation of O and H atoms into the grain and how the efficiencies vary with the temperature.

2 LABORATORY EXPERIMENTS

The experiments were performed with the FORMOLISM (FORmation of MOLecules in the InterStellar Medium) set-up. The apparatus is meant to study the reactivity of atoms and molecules on surfaces of astrophysical interest, under the conditions of temperatures and pressures similar to those in the ISM. The practicalities of the experimental set-up are described here but more details are given in previous works (Amiaud et al. 2007; Congiu et al. 2012).

2.1 Set-up

FORMOLISM is composed of an ultrahigh vacuum (UHV) stainless steel chamber with a pressure of a few 10^{-11} mbar. The main chamber hosts a sample holder that is located in the center and it is thermally connected to a closed cycle Helium cryostat. The temperature of the sample can be measured in the range of 10–800 K by a calibrated platinum diode connected to the sample holder. This one is made of a 1 cm diameter copper block (18 mm long). In the current set-up, we study the interaction and reactivity of oxygen and hydrogen atomic beams with a PAH-like surface, coronene, mimicking interstellar carbonaceous dust grains. Few layers of coronene ($C_{24}H_{12}$), contained in a movable crucible, are deposited on the sample holder held at 280 K. The movable crucible is placed at 3 cm in front of the sample holder and it works like an oven that heats up the solid powder. In our case, coronene (higher than 99 per cent purity; Sigma–Aldrich) is deposited on the surface by bringing the crucible up to 420 K to obtain a gentle sublimation. After the deposition the crucible is retracted into its own vacuum chamber. The obtained coronene film is a corrugated surface of disordered molecular clusters that mimicks typical dust particles with surface defects.

Two beams containing oxygen and hydrogen are aimed at the surface through a triple stage of differential pumping (three vacuum chambers connected together by tight diaphragms of 3 mm diameters). When the beams are sent to the surface, the overall pressure in the main chamber only rises by 1×10^{-11} hPa, and the partial pressure directly in the beam at the surface is estimated to be 2×10^{-8} hPa. Molecular pressures injected in the gas lines are about 1.5 mbar for the oxygen beam and 3 mbar for the hydrogen beam, and the atomic form of the beams is obtained by a microwave plasma discharge. However, after expansion in the source chambers, the pressure is immediately reduced to a few 10^{-5} mbar and so the atoms finally mostly interact only with the surface, after a free flight. The atoms are at a temperature slightly above the room temperature (<350 K), and they reach the surface at an angle of 40° for the hydrogen beam and 57° for oxygen, resulting in a reduced kinetic energy perpendicular to the surface.

For the detection, FORMOLISM is equipped with a quadrupole mass spectrometer (QMS). It allows both the detection of species desorbing from the sample during a temperature programmed desorption (TPD) and, when placed in front of the beam-line, the characterization and calibration of molecular beams, as well as the evaluation of the dissociation efficiency.

2.2 Detection methods

TPDs represent the most common experiments to determine the interaction energies and behaviour between chemical species and involved surfaces. These types of studies consist in selecting a system made up of a surface, coronene, on which a gas-phase species is sent, oxygen and hydrogen in our case. The latter would land, stick, react with incoming or already present species and further desorb, depending on the conditions. The temperature at which the surface is kept plays a crucial role. Every species (hydrogen, oxygen or newly formed molecules like water), have indeed a certain propensity to interact with the surface and to reside on it based on the surface temperature and binding energies. Once a specific temperature is reached, a given species can desorb, while at very low temperatures a species has enough residence time to stay on the surface, eventually diffuse and react with others forming new ones (in this work: water, O_2, and O_3). In our TPD experiments, coronene is cooled to temperatures ranging from 11 to 100 K and is exposed to oxygen and hydrogen beams. The interaction between the species and the surface can go from a simple, and lower in energy, physical adsorption to the formation of actual chemical bonds (chemisorption). Chemisorption is the only interaction mechanism that makes oxygen and hydrogen atoms stay on the surface at temperature above 40 K for a longer residence time, this enables further processes on the surface instead of sudden desorption. The eventual newly formed species, mainly water and O_3 in our study, will have a new binding energy with the surface and a new temperature of desorption. During our temperature-programmed desorption, coronene is heated over time with a linear ramp ($\beta = 12$ K min^{-1}) from an initial temperature (experiments from 11 to 100 K) to a higher one, 180 K, sufficient for the desorption of all the species in our system. Water molecules are the last ones to desorb at temperatures around 150 K. The signal of the desorbing species is detected by the quadrupole QMS in counts per second through the mass to charge ratio (m/z). The temperature at which each species desorbs, the shape and intensity of the peak, indicates the strength of the interaction (binding E), the type (order) of desorption and the amount of species undergoing that process.

Thus, TPDs are powerful tools to study the mechanisms of chemical reactions that occur on a specific surface and to infer the nature of the interaction between the surface and the adsorbing species.

The dissociation efficiency is instead measured by placing the QMS in front of the oxygen and hydrogen beams. The two beams do not interact with the surface in this case and this is just a measure of the amount of atoms that we are able to produce by dissociating the oxygen and hydrogen molecular beams. To evaluate the dissociation efficiency, we measure the drop in signal of the molecular mass, m/z = 32 for O_2 and m/z = 2 for H_2, and we observe a proportional increase of the signal of the atomic one, m/z=16 for O and m/z = 1 for H. The dissociation efficiency (per cent) for both the hydrogen and oxygen beams is usually stable over a day and we measure a typical value of 60 per cent for both beams.

2.3 Experimental protocol

This study focuses on exposing coronene to hydrogen and oxygen atomic beams in order to verify their respective and conjugated effect when they are sent on to the surface. In particular, we investigate the probability of the atoms being locked on the surface, how they physi- or chemi-sorb and/or if they promptly react with each other forming water molecules, or O_2 and H_2. The protocol is therefore divided into two main parts: preparation of the surface, with the collection of a reference, followed by an interaction of the surface with atomic oxygen and hydrogen beams. First, the coronene surface is formed by depositing it as described in Section 2.1 and afterwards cooled down to reach 10 K. At this point, to quantify the structure of the surface, its role as catalyst and the eventual changes due to the atomic irradiation, we use the molecular oxygen desorption peak as reference. This O_2 peak (after deposition of about 1 monolayer on the surface at 11–12 K) is taken everyday by detecting its desorption through the QMS with TPDs up to 50 K. The position (at a temperature of about 35 K) and shape of the O_2 desorption peak are well-studied in the literature and eventual changes can thus be an indication of surface alteration and evolution (Mohamed Ibrahim et al. 2022). This reference O_2 desorption peak is the black curve visible in Fig. 1 and it shows very little differences due to day-by-day changes on the coronene surface that, even if deposited by carefully controlling all the parameters, carries an experimental error. Once we are sure to have deposited the coronene and to have the reference for the day, we start with the second part of the protocol. Now, the following phase represents the actual investigation of the paper. Coronene, kept at a fixed temperature, is exposed to hydrogen and oxygen atomic beams for a certain time/dose. Right after the irradiation, the surface is cooled down to 10 K and at this point, we deposit molecular oxygen again to compare its desorption peak to the daily reference and to detect any changes to the surface due to the prior atomic irradiation. Therefore, after depositing about one monolayer of molecular oxygen, we perform the very final and most important TPD up to 180 K to detect the desorption peaks of O_2 just sent on the surface (green and magenta curves in Fig. 1, desorption T around 35 K), O_3 (green and magenta curves in Fig. 1, desorption T around 65 K), and water (blue and red curves in Fig. 1, desorption T around 150 K). The surface is subsequently cooled down to a given surface temperature, T_s, and a new protocol cycle can start.

At the beginning of the study, we have mainly focused on determining the effects for surface temperatures of 11 and 45 K, Fig. 1. Afterwards we have examined different times/doses (see Fig. 2) for these same two temperatures in order to define the best one suitable for comparing different temperatures. Finally, we have evaluated the amount of water formed through the O and H atomic irradiation of coronene kept at fixed temperatures ranging from 10 to 100 K for the chosen time/dose (30 min), Fig. 3. The last but very important detail regards the two different approaches used right after the irradiation, and before the O_2 deposition to check the surface changes, for temperatures below and above 35 K. Since the molecular oxygen coming from the undissociated part of the beam sticks on the surface during the irradiation for temperatures below 30 K, this one is removed after the irradiation and before any further analysis by heating the surface up to 50 K. This allows us to verify only the effect from the atomic beam and to have the same conditions for experiments at all temperatures. Once the irradiation is finished and we have eventually removed the O_2 stuck on coronene for temperatures below 35 K, the surface is cooled down to 10 K to deposit 1ML of O_2 for the daily reference comparison and the protocol follows the general description given above.

To sum up, all the experiments presented here consist in depositing the coronene surface every day before any set of experiments (typically 1–3 cycles of water formation, without substantial changes to the coronene), collecting a O_2 reference, atomically irradiating the surface and checking its changes through the molecular oxygen peak, lastly recording the molecules formed though TPDs up to 180 K. With the QMS, the same molecule can be detected with different m/z ratios corresponding to the fragmentation of the parent molecules after the electron impact (here at 30 eV). The main fragments under

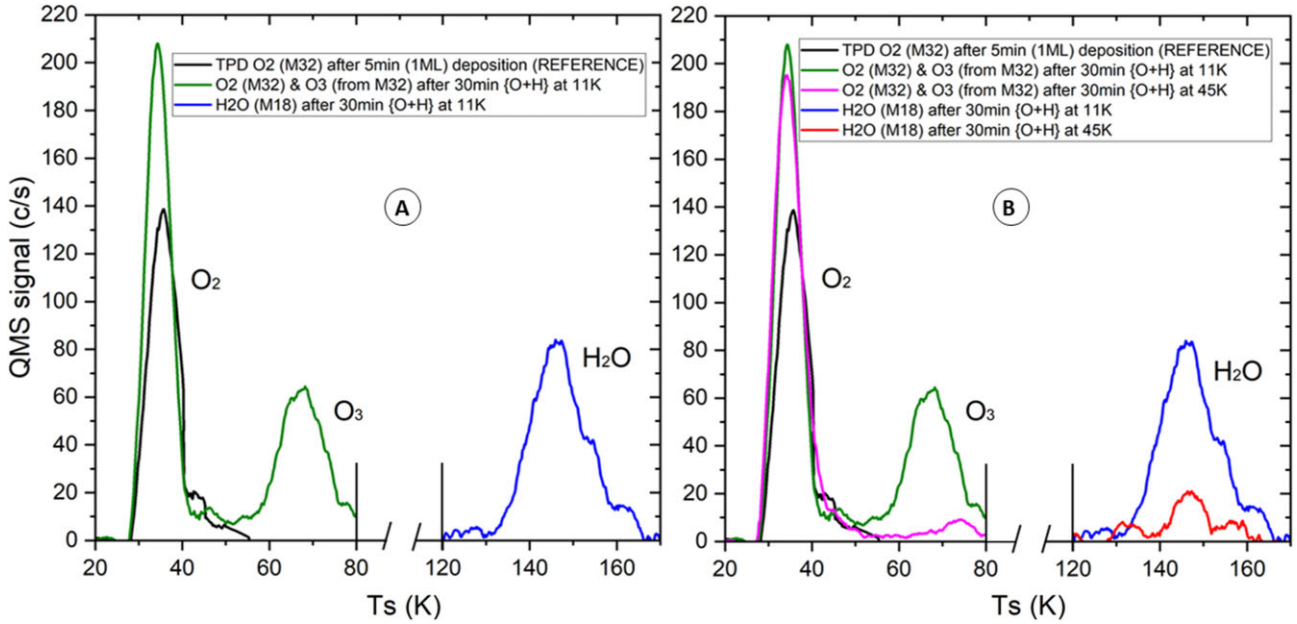

Figure 1. (A) Black curve: O_2 reference peak; green curve: O_2, of about 1ML deposition added after irradiation, and O_3 from 30 min $\{O + H\}$ exposure at 11 K; blue curve: H_2O from 30 minutes $\{O + H\}$ exposure at 11 K. (B) Black curve: O_2 reference peak; green curve: O_2, of about 1ML deposition added after irradiation, and O_3 from 30 min $\{O + H\}$ exposure at 11 K; blue curve: H_2O from 30 min $\{O + H\}$ exposure at 11 K; magenta curve: O_2, of about 1ML deposition added after irradiation, and O_3 from 30 min $\{O + H\}$ exposure at 45 K; red curve: H_2O from 30 min $\{O + H\}$ exposure at 45 K.

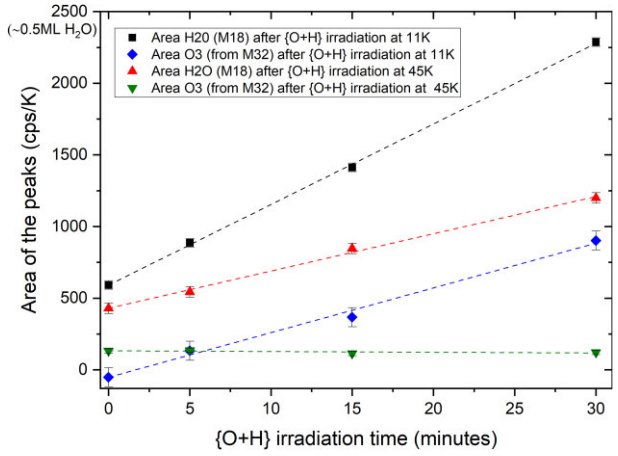

Figure 2. Area of O_3 and H_2O peaks after several irradiation times (0, 5, 15, and 30 min) at 11 and 45 K. The error bars are obtained from the linear regression.

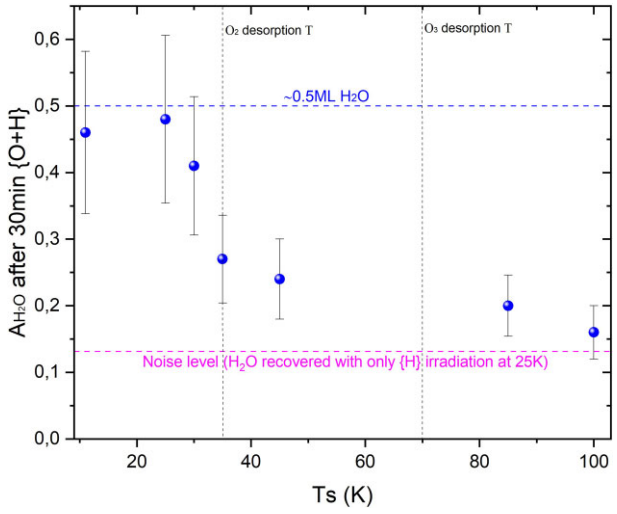

Figure 3. Area of H_2O after 30' irradiation dose at 11, 25, 30, 35, 45, 85, and 100 K normalized to 1ML H_2O Area on coronene. The error bars represent the standard error from standard deviation.

study here are m/z = 2 (molecular mass of H_2), m/z = 18 (molecular mass of H_2O), m/z = 32 (molecular mass of O_2 and main fragment of O_3), and m/z = 48 (molecular mass of O_3).

3 RESULTS

All the results shown in the following paragraph come from theTPD experimental method, as described in the protocol. The idea is to check both the changes produced on the surface when the atoms are sent and, most importantly, the amount and type of molecules (namely O_2, O_3, and H_2O) formed.

3.1 Experiments at 11 K

In Fig. 1(A), we show the TPD peaks recorded by using the QMS for the first part of this study. The surface is kept at 11 K and two types of analyses are performed here. First, we collect the reference peak of about 1 ml (monolayer) of O_2 [referred to as mass 32 (M32), see black curve] to have the position (desorption temperature/binding E) and the shape of O_2 interacting with coronene. Secondly, and separately, the surface is exposed simultaneously to hydrogen and oxygen atomic beams for 30 min, before detecting the desorbing species with the TPD method. The main molecules under analysis here are molecular oxygen, O_3, and water molecules. As shown in Fig. 1(A), O_2 is characterized by a desorption peak at around

35 K (m/z = 32 reference peak, black curve). In Fig. 1(A), we also observe the other two main products of the {O+H} exposure: ozone, O_3, (from the m/z = 32 fragment signal, green curve) with a TPD peak around 70 K and water molecules (m/z = 18, blue curve). H_2O is the one desorbing at the highest temperatures in our system, as shown by its peak centered at 150 K. By checking the behaviour of M18 (m/z = 18) during the TPDs, we observe a peak at higher temperatures only for the experiments at 11 K. The water peak also represents the main fragment of the H_2O_2 molecule and we do see a sign of its desorption around 177 K only when O and H atoms are sent on to the coronene at 11 K. This is in agreement with previous works studying water formation at very low temperatures (Ioppolo et al. 2008; Chaabouni et al. 2012). In fact, at temperatures around 10 K, O_2 represents a stable and largely available reactant whose chemistry also leads to the formation of H_2O_2, as reported in the introduction. The reactivity of O_2 towards the formation of H_2O_2 becomes less relevant at higher temperature due to its mobility on the surface, by approaching its desorption temperature, and the appearance of a more relevant O_3 chemistry with an overall water formation being favoured instead.

In Fig. 1, one can notice how the amount of molecular oxygen desorbing from the 1 ml deposition realized after irradiation (green and magenta curves) is consistently higher than the reference peak (black curve). The most simple explanation relates to the actual higher quantity of O_2 deposited in the same 5 min, that are usually used as reference. Since this deposition is realized after the atomic irradiation, during which the plasma is turned on, the molecular flux tends to be higher when compared to the conditions prior to the {O+H} exposure. Even after waiting a certain time for all the parameters and pressure to be back to the initial conditions, there is a trend in all experiments that shows an average of about 30 per cent of more molecular oxygen coming from the surface with respect to the reference peak. The actual flux after atomic irradiation is therefore depositing more O_2 than expected. Since we are controlling, with the time/dose and pressure we are using, the deposition of about 1 ml of O_2 only, even if we observe the desorption of a higher quantity, we keep referring to these reference peaks as the desorption peak of the deposition of about 1 ml of O_2. This does not have an impact on the analyses and on the interpretation of the results. To this main factor, one has to add the possible change in sticking coefficient because the surface is now hosting the newly formed species, namely ozone and water. In Fig. 1(A), as expected at 11 K, the molecular part of the oxygen beam is sticking on the surface during irradiation, allowing all the three mechanisms for water formation described in the introduction. The first formation route (O+H path) is the most obvious, but also the presence of O_2 during the plasma exposure allows, given a certain degree of dissociation, the formation of O_3 and its further hydrogenation, as well as the reaction of O_2 with the incoming H atoms. Also, one would expect that at these low temperatures the direct interaction of atomic oxygen and hydrogen mediated by coronene would result in a reaction that forms water with a 100 per cent efficiency, while only a part of our system goes in this direction. The explanation is due to the hydrogen being the limiting reactant, allowing the rest of O to recombine as O_2 or to form O_3.

The black curve, reference O_2 peak, is mostly used to compare the effect of the {O+H} exposure on the coronene surface. The goal is to check if there is evidence of a relevant position shift (different desorption temperature and therefore different binding E) and shape of the molecular oxygen peak after the {O+H} irradiation (green curve). No relevant variation from the reference of the O_2 peak is observed here.

3.2 Experiments at 45 K

So far we have presented and introduced the topic by using the results obtained at widely studied low temperatures, 11 K in our case, where the expected reaction pathways are very efficient. Fig. 1(B) shows, by following the same protocol of Fig. 1(A), also the results when the coronene surface is kept at 45 K during the {O+H} exposure. The main point here is to check the surface temperature effect on the quantity of O_3, magenta curve, and H_2O, red curve, formed. At temperatures higher than 35 K, molecular oxygen does not accumulate on the surface anymore, since it instantaneously desorbs upon sticking, limiting its contribution in forming O_3 and further water formation pathways during the atomic exposure. The O+H reaction route is happening in both cases (at 11 and 45 K), with an evident and obvious higher efficiency at 11 K. All those effects result in a noticeable higher quantity of water synthesized on the grain during {O+H} irradiation at 11 K. The predictable and almost negligible amount of O_3 at 45 K is not surprising, but the presence of formed water represents here the novelty of this study. Thus, the fact that there is still a quantifiable amount of H_2O formed at 45 K stimulated us in this study to search for higher temperatures at which the system {O+H}-coronene would still produce a reasonable amount of water.

3.3 Temperature effect

Fig. 2 displays the effect of different {O+H} doses and the comparison for temperatures below and above the O_2 desorption (around 35 K). Every point on the graph represents the integrated areas under each respective peak. The first thing to notice is a good proportionality found for the area of the H_2O peaks with increasing doses of {O+H} at both 11 and 45 K. The most efficient water formation pathway, in terms of quantity recovered, is as expected happening at 11 K, with twice the efficiency with respect to the same atomic irradiation method at 45 K. Again, at 11 K all the water formation routes are open. The other remarkable point is the proportionality of O_3 formation at 11 K and the absence of variation detected at 45 K, underlining the important role of the sticking of O_2 molecules on coronene for its formation and their eventual hydrogenation to form water. Last but not least, this plot allows to choose the best dose to use to further compare the behaviour at different temperatures. The 30 min time-dose is found to be a reasonable reference in order to maximize the amount of water recovered from the surface before having too many molecules covering it and therefore reducing the effect from the coronene surface itself. The maximum amount of water formed on coronene is in fact obtained for the 30 min deposition at 11 K, but it stays right below 1/2 ml, ensuring the exposure of the surface to the incoming beams. To determine the area of 1 ml of water on coronene, we have deposited 30 ml of ice film on the coronene surface by using a separate channel and a micro-capillary array doser, keeping the pressure of the main chamber always below 10^{-8} mbar, as reported in previous work (Ferrero et al. 2022). The value has been confirmed by comparing it to the area of about 1 ml of water deposited on coronene, which differs only 13 per cent. The 30 min dose is afterwards also used to compare the effect and the results from exposing the surface with the O and H beams together, up to 100 K, alone or in sequence at $T_s = 25$ K.

Fig. 3 shows the integrated values of the water peaks detected after irradiating the surface with the {O+H} beams during 30 min at temperatures up to 100 K. The reported values are normalized with respect to the area of about 1 ML of water on coronene. A stable and

maximum situation is obtained for temperatures up to 25 K, while the first decrease of the plot is observed between 30 and 35 K. After 35 K the amount of water formed with {O+H} irradiation already reaches a lower value that extends up to 85 K, with a non-negligible area still at 100 K, even if the calculated error bar already falls in the noise level. The molecular oxygen from the undissociated beam, and the newly formed one through recombination, can stick and remain on the surface upon irradiation at temperatures lower than 35 K, as shown by the first dashed vertical line in Fig. 3. During the {O+H} exposure, the presence of O_2 therefore helps in forming O_3 and water, with the advantage of a longer residence time for the atoms at those temperatures. This results in an overall more efficient water formation pathway when the coronene is kept at temperatures up to 35 K: all the main three formation routes are possible. Between 35 and 70 K there is no O_2 staying on the surface anymore, but the formed O_3 and the incoming oxygen and hydrogen atoms still provide an efficient water formation on coronene. After 70 K, second dashed vertical line, O_3 desorbs and does not contribute anymore to form water through its hydrogenation. This is when only the O+H route is available and we observe the lowest water formation efficiency. The bottom magenta line displayed in Fig. 3 represents the integrated area of the water peak when only H atoms are sent onto the surface, at 25 K. In this conditions the water could only come from the beam, as a pollutant, or from the chamber and it is not due to the {O+H} interaction. Its level is thus taken here as a minimum noise level. However, Fig. 3 confirms the important role played by coronene and the temperature dependence of the system under study in this paper, as well as the important role of the O_2 and O_3 molecules. The fact that water is formed at temperatures higher than 40 K proves the chemisorption of O atoms on coronene, since they would otherwise never be present on the surface for further reactions at those temperatures. The chemically adsorbed oxygen atoms therefore represent available reactants for the incoming O, O_2, and H to undergo all the possible reactions.

3.4 Catalytic role of coronene

Our experimental results provide further evidence to the catalytic role of coronene in these types of systems, already observed in previous work from our group for H_2 recombination (Grieco et al. 2023). As already discussed above, coronene represents an efficient catalytic surface for water formation up to 85 K when O and H atoms are sent together. In the following section, we study the role of the surface when the atomic beams are sent separately or in sequence and we compare the different results in order to understand the mechanisms involved.

Fig. 4 reports the amount of O_2, O_3, and H_2O recovered after each irradiation. All of them were obtained by exposing the surface to the hydrogen and oxygen beams together [{O+H}), separately ({O} and {H}) or in sequence ({O}+{H} and {H}+{O}), at 25 K. Since the experiments displayed in Fig. 4 are carried out at a temperature below the desorption one of O_2, the integrated area of the oxygen peak shown here represents the actual molecules stuck on the surface, coming from the undissociated part of the oxygen beam as well as the ones eventually formed by atomic recombination, that have not resulted in water formation. The most H_2O is detected for the {O+H} exposure (black histogram) since, as expected, when hydrogen and oxygen atoms are sent together towards coronene, they can promptly react and undergo all the possible pathways. In this case, hydrogen represents the limiting factor for a full water transformation, this is why we still observe a certain amount of O_2 and O_3. One has also to consider that a part of the newly formed water could have been returned to the gas-phase through chemical desorption. In fact, by comparing the total oxygen recovered when only oxygen atoms are sent to coronene ({O}, blue histogram) with the black histogram ({O + H} exposure), one can indeed conclude that more or less 1/3 of the overall oxygen is recovered when O and H atoms are sent together and only 1/6 of it is observed in the form of water desorbing from the surface.

The most O_2 is instead detected when coronene is exposed to only oxygen atoms ({O}, blue histogram). In this case in fact, except for the hydrogen that can be found on the surface or abstracted from it, oxygen atoms act alone in order to recombine (highest O_2 value in Fig. 4) or to form O_3 with the available molecular one. As expected, this is when the smallest amount of water is formed.

On the other hand, the experiment with only hydrogen atoms ({H}, magenta histogram) irradiating the surface allows us to have an idea of the role of the surface in water formation and to be sure that the oxygen beam is the only source of O atoms in our system. No O_2 or O_3 are indeed recovered from the surface in these conditions, while there is a certain amount of water desorbing even after this experiment. It has to be considered that water could come from the beams as a pollutant or was already be present as a low background in the chamber. For this reason, the amount of water desorbed when only H atoms are sent on to the surface for 30 min at 25 K are taken in this study as the noise level (see Fig. 3). Finally, we have investigated the effect of exposing coronene to the hydrogen and oxygen beams in sequence, therefore separately, and not together. In Fig. 4, we show the two possible cases: when the 30 min exposure of oxygen atoms happens before the hydrogen one ({O}+{H}, red histogram) and the reverse situation ({H}+{O}, green histogram). In the first case, red histogram, we observe the second highest amount of water detected out of all the experiments, after {O+H}. A temperature of 25 K ensure in fact a residence time long enough to stabilize an interaction oxygen–coronene that will make the atoms available on the surface for the H atoms that are only going to be sent afterwards. However, since the amount of water is lower than the {O+H} experiment, we observe a larger amount of oxygen transformed into O_2. The maximum amount of O_3 is instead detected for the reverse experiment: {H}+{O}, green histogram. Contrary to what happens when oxygen atoms are sent before the H ones, in this case 25 K is a temperature already too high for the hydrogen atoms to reside on the surface long enough for the afterwards incoming O. For this experiment, the amount of water observed can be explained similarly to the {O} case.

All the results shown in this paper are therefore of extreme importance for a better understanding of water formation on carbonaceous dust grains at temperature up to 85 K, the role of a PAH-like surface at different temperatures and the effect of the interaction of oxygen and hydrogen atoms with coronene.

4 ASTROPHYSICAL IMPLICATIONS

The main results from this paper are (1) the formation of water on PAH-like carbonaceous surfaces for temperatures up to 85 K and (2) the catalytic role of coronene. To understand the astrophysical importance of these findings we have to focus on the ISM phases where this could be relevant: the presence of PAHs, the physical conditions, such as the grains temperature, and the availability of O and H atoms.

4.1 Water formation at high temperatures

Talking about the high-temperature formation of water on dust grains, one should zoom into the ISM regions right before the onset of the ice mantle (A_V = 0–3). In these regions there are wide temperature

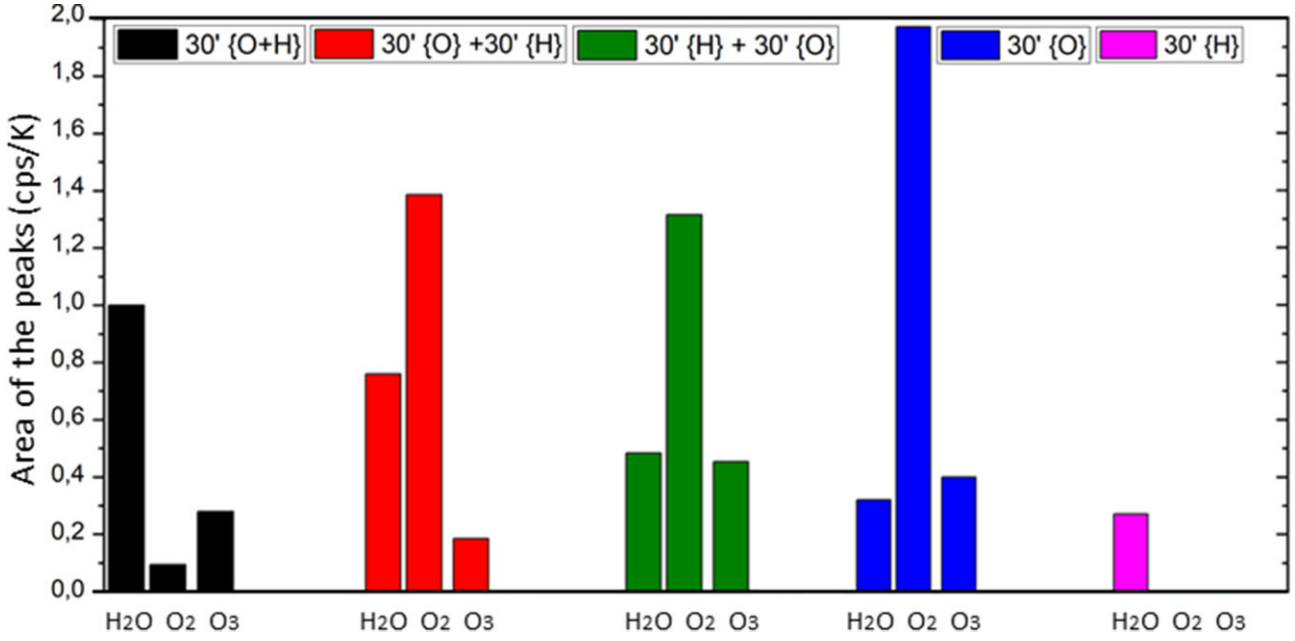

Figure 4. O_2 (from the irradiation, M32), O_3 (M48), H_2O peaks Area after {O+H} 30' irradiation at 25 K normalized to Area of H_2O recovered from the 30' {O+H} exposure.

ranges, with values higher than the ones so far believed to be important to form water on grains and for ice mantle formation (Corby et al. 2018). The temperature drops going towards denser regions reaching conditions widely studied and accepted. At lower T, around 10 K, the catalytic effect of the PAH surface no longer plays an important role, since the grains start to be covered in layers of ice. In these conditions new ice layers will form on top of the pre-existing ones and we only observe a thickening of the ice mantle. The observed ice abundances are in fact generally in agreement with considering water formed by atomic accretion from the gas-phase followed by grain surface chemistry. From observations, the ice mantle formation threshold is believed to be around $A_V = 1.6$, near local cloud edges, and this is actually taken as the onset of rapid ice mantle growth after a first monolayer has formed (Hollenbach et al. 2009). In fact, as stated in the introduction, in regions with A_V higher than 2, therefore in the so-called transition zones, it is more difficult to assess whether PAHs exist, as small grains or incorporated in the already existing icy mantles (Boogert, Gerakines & Whittet 2015). The actual reasons behind the disappearence of typical PAHs features from detection represent the many question marks about this phenomenon. *JWST* will for sure help in studying PAH abundances and give more details about different environments. As said before, coronene is one of the most stable and least reactive PAH species and, from the results obtained in this study, there is not enough evidence and experimental accuracy to exactly asses the eventual O or H lockup in the grain, while a prompt reaction to form H_2O is surely favoured instead. Water could start covering the surface at higher temperatures than considered before.

This process could have a relevant impact on the formation of other molecules whose formation depends on icy grains and their surface temperature. Many molecular reactions happening on dust grain icy mantles are indeed strongly temperature dependent, even if the ice does not exactly participate as a reactant itself. The most interesting ice-dependent species are complex organic molecules (COMs). They can form as by-products from the ices or by combination of photo-processing with UV photons penetration. In fact, some COMs are thought to be formed in translucent conditions where the built of ice mantles combines with an external UV field. In particular, some studies have focused on how these reactions and conditions could be relevant for new surface/ice reactions involving CH and CH_2. Other two COMs involved in energetic ice formation pathways are formamide and acetaldehyde (Whittet 2010; Martín-Doménech, Öberg & Rajappan 2020). The earlier set of ices on dust grains discussed in this paper would involve regions where higher temperatures and the presence of UV photons could have an effect on the formation of those molecules. Many aspects discussed in this section are summarized in Fig. 5, that is here used to give a better idea of the regions in which the formation of water up to 85 K can be relevant: T_{grains} = 10–100 K, $0 < A_V < 3$ and a certain availability of oxygen and hydrogen atoms. Given the efficiency by which O atoms are transformed into water as soon as H atoms appear, and in the presence of catalytic surfaces such as PAHs, these regions could represent a perfect candidate for such reaction. For A_V lower than 1, where we actually have T_{grains} around 85 K, the eventually formed water is immediately injected into the gas-phase, where it can undergo photodestruction ($K_{H_2O^*}$ in Fig. 5 represents indeed the ratio between its formation and photodestruction). After the H/H_2 front, water molecules remaining on the surface could start covering the grains by forming the very first sub-layers before the ice mantle regime ($A_V = 3$).

4.2 Hydrogenation and functionalization of PAHs

In UV dominated zones (diffuse to translucent clouds, up to boundaries of dark clouds), proof has been found of hydrogenated PAH (Le Page, Snow & Bierbaum 2003, 2009) and it would be very useful to also assess the presence of functionalized PAH that would eventually lead to water formation. In interstellar regions with number $>10^4$ cm^{-3}, the O+H route seems to be crucial, it is thus reasonable to consider these reactions as relevant in environments where UV photons and atomic species dominate. In diffuse clouds and boundaries of the dense ones, $A_V < 3$, the O+H reaction route may be the only process

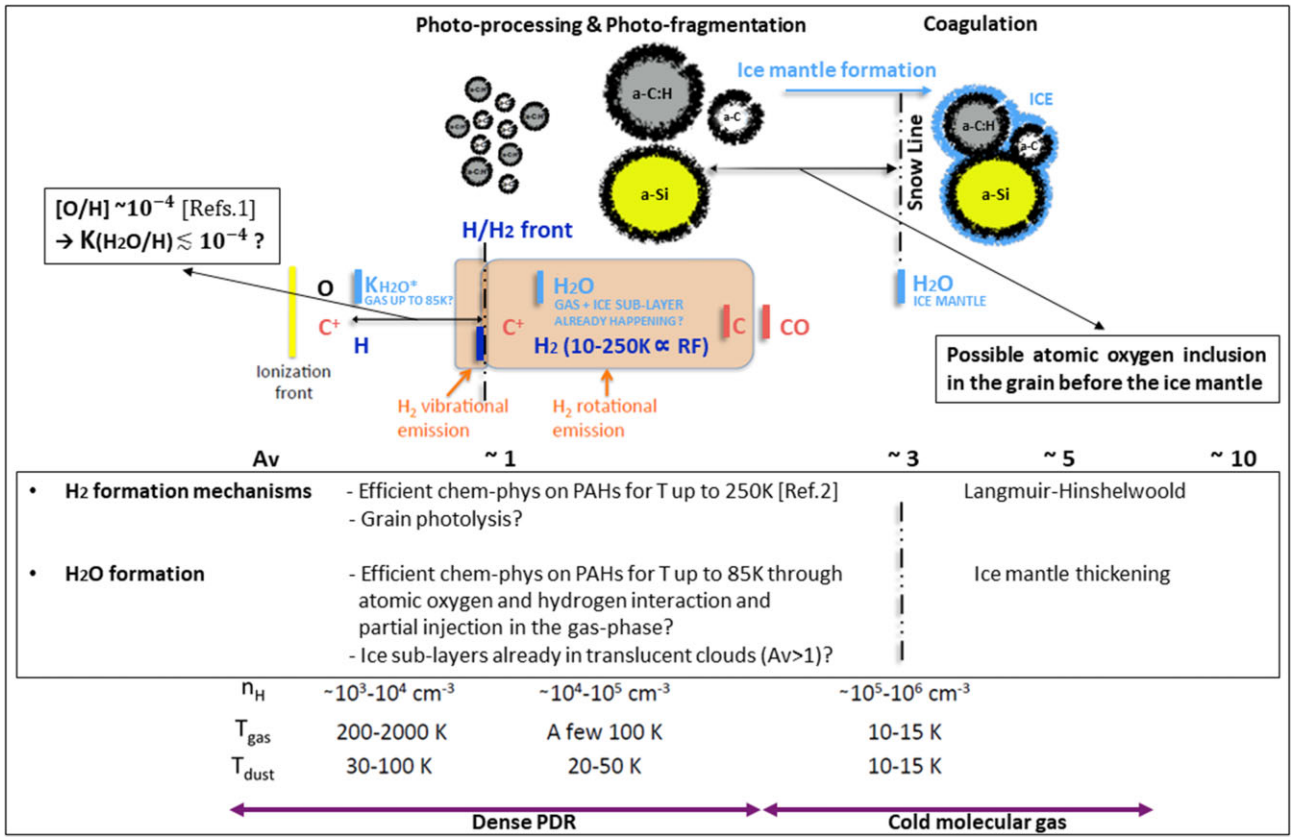

Figure 5. Summary schematic illustration of the main H_2 and H_2O formation processes in PDRs including the results of this study. Updated version of the scheme taken from Wakelam et al. (2017). *References* 1: Fuente et al. (2019), Laas & Caselli (2019). 2: Grieco et al. (2023).

for the efficient formation of the first monolayer of water ice on bare interstellar grains. Specifically, in regions with low UV flux PAHs are expected to be mainly neutral and possibly superhydrogenated (Allamandola, Tielens & Barker 1989; Le Page, Snow & Bierbaum 2003). Even hydrogen already adsorbed or present on the surface could contribute in further hydrogenation of the newly formed OH. Rauls & Hornekær (2008) and Jaganathan et al. (2022) report the possible oxygen-functionalization of PAHs where a subsequent H addition leads to the loss of the oxygen-functional groups via the formation of small oxygen-containing species such as water. There is experimental evidence for the enhanced reactivity of oxygen-functionalized PAHs as compared to their pristine analogues. The fast reaction with incoming H atoms could represent an explanation for why oxygen-functionalized PAHs are more elusive in the ISM gas-phase (Dulieu et al. 2019). If the temperature of the system is below the desorbing temperature of water molecules in fact, the newly formed OH may remain on the grain forming ices.

PAHs are assumed to have an important role in providing a catalytic surface for reactions in the ISM, but they can also play a role in water formation and therefore ice formation extending the range of temperatures than previously thought. If we take into account the results of our work, for temperatures below 100 K this could already be happening. Regions characterized by $A_V < 3$, presence of atomic oxygen and hydrogen as well as neutral or superhydrogenated PAHs with temperatures higher than few tens of K, could therefore be the perfect conditions for the results presented in this paper, as summarized in Fig. 5. So far, the formation of water on a grain has been mainly considered at temperatures around 10 K in cool or dense clouds, and there are studies about its formation at maximum 40 and 50 K. The results reported here extend the temperatures of interest and could give new answers on why PAHs seem to disappear in transition zones by considering higher temperatures for the formation of ice in the ISM. Also, this study confirms and underlines the catalytic role of PAHs for the formation of small molecules such as H_2 and H_2O. If water can be formed by hydrogen and oxygen addition on PAHs, eventual water-PAH complexes could also lead to CO_2 formation driven by UV photons, as reported by the study of Potapov, Jäger & Henning (2019).

4.3 Evidence of grain growth

Another question of this project has been the possible lock up of oxygen into the carbonaceous grain, contributing to its growth and being a possible explanation for O depletion. In our conditions, by using coronene and at a given experimental accuracy, it is not possible to easily assess whether oxygen is locked up in the surface. In order to verify the eventual inclusion of oxygen atoms in the grain we checked the surface with O_2 peaks after the irradiation, see green and magenta curves in Fig. 1, and compared them to a reference taken before any modification. In order to study a possible evolution or morphological changes in the surface structure, we were aiming to see a certain change in the shape and/or position of the peak, in addition to recovering M16 or M32 (respectively m/z = 16 for O and m/z = 32 O_2) together with the desorption of coronene from the sample holder (at around 300 K, m/z = 300). We have not observed a release of atomic or molecular oxygen upon surface desorption. The O_2 peak method has been used also to check the surface after irraditions up to 100 K, not only for 11 and 45 K as shown in Fig. 1. In all cases, we only observe a trend for the peaks to shift towards slightly higher temperature when less water is

formed (higher temperature for the {O+H} exposure). In addition, our experiments are hampered by an uncertain input flux as suggested by the higher depositing flux for the O_2 peaks after irradiation (see Section 3.1). Due to additional possible changes in the sticking coefficient and the complex surface chemistry involved, it is not trivial to assess whether oxygen is locked up in the grain. Given the strong catalytic role of PAHs and the fact that we do not see any M16 or M32 desorbing with coronene, it is possible that oxygen has not been locked up in our surface, therefore there is no direct sign of grain growth. Coronene-like structures could not be adequate surfaces, but also the experimental study of the oxygen depletion problem and grain growth seem to carry a very high complexity. Coronene corresponds in fact to a very small and stable structure that does not easily accumulate atoms or molecules inside. In our case, we observe how oxygen atoms suddenly react with the always available H atoms forming ices. There have been theoretical studies (Jones & Ysard 2019) about the role of atomic O interacting with a-CH mantles of grains aiming to explain the disappearance of oxygen in the denser ISM, or what they would define an 'anomalous incorporation of oxygen into dense ISM'. These doubts arise since the depletion of O, 40 per cent of the overall abundance (170–255 ppm) (Whittet 2010), is faster than incorporation into dust. They suggest incorporation of O into a-CH mantles to form epoxides and carbonyls. The latter functional groups can further react with CO_2 and O to finally give cyclic organic carbonates. Organic carbonates would thus solve the problem and explain the elemental abundances/depletions and ratios involved; they should form in the translucent ISM before ice mantles (Jones & Ysard 2019).

There are other relevant works trying to address the oxygen depletion problem. Poteet, Whittet & Draine (2015) investigate if in the diffuse to dense cloud transition zone there is a chance for the missing, or not easily observable, oxygen to be locked up in big O-bearing grains opaque to IR radiation. Another option that they consider is the possibility of thick H_2O ice mantles being an important reservoir of oxygen as well. Those two solutions could both lead to an explanation for the missing oxygen, but only future observation can shed light on these hypotheses. Wang, Li & Jiang (2015) consider instead the possibility of having μm-sized H_2O ice grains formed in dense clouds, but still present in more diffuse environments before being photo-sputtered. For both cases, the results of this paper could support the hypothesis that forming water ice at warmer temperature could either contribute to the formation of an eventual thicker ice mantle or to the existence of μm-sized ice grains before very dense environments. In Fig. 5, apart from stressing on how the results of this paper could be crucial to understand the catalytic formation of water on PAHs up to 85 K, we also point out that a possible inclusion of oxygen atoms in the surface could happen only before the onset of the ice mantle. However, the formation of ices at higher temperatures than previously thought can still be considered to contribute to the explanation of O depletion. Also, in conditions where H atoms are so abundant, their interaction with oxygen through a PAH surface would most probably lead to water molecules formation rather than O atoms inclusion in the structure. Finally, we want also to acknowledge how the results provided in this paper could be used to help answering new questions in other fields. The formation of water on carbonaceous grains at temperature higher than so far demonstrated could help understanding why H_2O would remain frozen in relatively warm environments. This could give new insights in the study of snowlines in protoplanetary discs (Tinacci et al. 2023).

This study, even if it is not providing answers or supporting the organic carbonate route in the case of coronene and possible grain growth, confirms the role of small and stable PAH-like structures as catalysts. It opens the door to further experiments that should focus on surfaces that could more easily incorporate atoms into their structures and be more easily functionalized in order to assess grain growth and interstellar elemental depletions.

5 CONCLUSIONS

In this paper, we provide experimental evidence of water molecules forming on a PAH-like surface by oxygen and hydrogen accretion from the gas-phase at temperatures up to 85 K. This study represents another crucial experimental proof of carbonaceous surfaces being efficient catalysts.

In a previous study from our group, we have reported new results that extend the H_2 formation temperatures up to 250 K, when coronene is used as surface. We demonstrated the possibility of chemisorption as an explanation for the H atom recombination on coronene at high temperatures (Grieco et al. 2023). The same happens in this set of experiments when O and H atoms are sent to the surface. All three mechanisms leading to water formation can happen in our conditions, with different probabilities and efficiencies depending on the temperature at which the surface is kept. About 1/2 ml of water is formed and detected for temperatures around 20 K with 30 min {O+H} coronene exposure, and a non-negligible amount above the noise level is still recovered at 85 K. Thus, also in this case, as for H_2, coronene plays a very important catalytic role.

Chemisorption is the phenomenon that would explain why O and H are still on the surface and react at temperatures above 40 K. Temperatures at which atoms start to desorb are usually very low if only physical bonds are involved while here we observe the resilience of the atoms staying on the surface at higher temperature to further react or recombine. This is a typical example of chemisorption where the stabilization happens through actual chemical bonds that need higher energies/temperatures to be broken and result in the desorption of the species. This naturally has a direct effect on the residence time and it gives more chances to go through other processes while being on the surface. In our system O atoms can chemisorb on the surface forming O_2 and O_3, as well as OH and finally H_2O as soon as H atoms appear.

In our conditions, we indeed observe how water formation is extremely favoured, but we are not able to precisely asses an eventual atomic lockup in the surface resulting in grain growth, functionalization or morphological change by only using a reference O_2 peak as a probe.

Here, we also want to mention the importance for these results to be taken into account for future and/or ongoing *JWST* projects in characterizing PAHs to be eventually combined with H_2O observations in order to study their potential impact on its formation at warm temperatures. There are already some first *JWST* results by the PHANGS (Physics at High Angular resolution in Nearby GalaxieS) group studying the changes, over three nearby galaxies, of the average PAH sizes as well as their ionization state. They report regions with hotter PAHs and a more important heating/change in PAH size correlation with higher molecular gas content (Chastenet et al. 2023). Future studies on PAH characterization by mapping their sizes, temperature, and ionization state in different regions could help to further understand their role for physical–chemical processes happening on dust grains and eventually support the warm temperature formation of H_2O on those catalytic surfaces.

Considering the stability of coronene and the ability to stabilize species to further making them react, we can conclude on its incredible catalytic role and extend the range of temperatures for the formation of water. We stress that also the potential formation of other molecules on carbonaceous grain surfaces at high temperatures should be considered in the future.

ACKNOWLEDGEMENTS

This work has been funded by the European Research Council for the Starting Grant 'DustOrigin', held by Prof. Ilse De Looze, University of Ghent, grant agreement ID number 851622. It was supported by the Agence Nationale de la Recherche (ANR) SIRC project (grant number ANR-SPV202448 2020-2024). We thank colleagues from LERMA-CYU for their support and especially the engineer of the set-up Dr. Saoud Baouche.

DATA AVAILABILITY

Metadata have been created on the laboratory platform. Files are automatically released after 3 years from the uploading date. The data that support the findings of this study are available from the corresponding author upon reasonable request.

REFERENCES

Allamandola L. J., Tielens A. G. G. M., Barker J. R., 1989, ApJS, 71, 733
Amiaud L., Dulieu F., Fillion J. H., Momeni A., Lemaire J. L., 2007, J. Chem. Phys., 127, 144709
Bernstein M. P., Sandford S. A., Allamandola L. J., Gillette J. S. B., Clemett S. J., Zare R. N., 1999, Science, 283, 1135
Boogert A. C. A., Gerakines P. A., Whittet D. C. B., 2015, ARA&A, 53, 541
Bouwman J., Mattioda A. L., Linnartz H., Allamandola L. J., 2011, A&A, 525, A93
Caselli P. et al., 2010, A&A, 521, L29
Ceccarelli C., Caselli P., Herbst E., Tielens A. G. G. M., Caux E., 2007, preprint (arXiv:astro-ph/0603018)
Chaabouni H. et al., 2012, J. Chem. Phys., 137, 234706
Chastenet J. et al., 2019, ApJ, 876, 62
Chastenet J. et al., 2023, ApJ, 944, L12
Cleeves L. I., Bergin E. A., Alexander C. M. O. D., Du F., Graninger D., Öberg K. I., Harries T. J., 2014, Science, 345, 1590
Congiu E., Chaabouni H., Laffon C., Parent P., Baouche S., Dulieu F., 2012, J. Chem. Phys., 137, 054713
Cook A. M., Ricca A., Mattioda A. L., Bouwman J., Roser J., Linnartz H., Bregman J., Allamandola L. J., 2015, ApJ, 799, 14
Corby J. F., McGuire B. A., Herbst E., Remijan A. J., 2018, A&A, 610, A10
Cuppen H. M., Herbst E., 2007, ApJ, 668, 294
Dulieu F., Amiaud L., Congiu E., Fillion J. H., Matar E., Momeni A., Pirronello V., Lemaire J. L., 2010, A&A, 512, A30
Dulieu F. et al., 2014, 40th COSPAR Scientific Assembly , 40, F3.2
Dulieu F., Morisset S., Ibrahim Mohamed A.-S., Boshman L., Cazaux S., Teillet-Billy D., Baouche S., Rougeau N., 2019, Mol. Astrophys., 17, 100054
Ferrero S. et al., 2022, MNRAS, 516, 2586
Ferullo R. M., Zubieta C. E., Belelli P. G., 2019, PCCP (Incorporating Faraday Trans.), 21, 12012
Fuente A. et al., 2019, A&A, 624, A105
Grieco F., Theulé P., De Looze I., Dulieu F., 2023, Nat. Astron., 7, 541
Gudipati M. S., Yang R., 2012, ApJ, 756, L24
Guennoun Z., Aupetit C., Mascetti J., 2011, PCCP (Incorporating Faraday Trans.), 13, 7340
Hollenbach D., Kaufman M. J., Bergin E. A., Melnick G. J., 2009, ApJ, 690, 1497
Ioppolo S., Cuppen H. M., Romanzin C., van Dishoeck E. F., Linnartz H., 2008, ApJ, 686, 1474
Jaganathan R., Simonsen F. D. S., Thrower J. D., Hornekær L., 2022, A&A, 663, A136
Jensen S. S., Jørgensen J. K., Kristensen L. E., Furuya K., Coutens A., van Dishoeck E. F., Harsono D., Persson M. V., 2019, A&A, 631, A25
Jochims H. W., Baumgärtel H., Leach S., 1999, ApJ, 512, 500
Jones A. P., Ysard N., 2019, A&A, 627, A38
Kristensen L. E., Amiaud L., Fillion J. H., Dulieu F., Lemaire J. L., 2011, A&A, 527, A44
Laas J. C., Caselli P., 2019, A&A, 624, A108
Le Page V., Snow T. P., Bierbaum V. M., 2003, ApJ, 584, 316
Le Page V., Snow T. P., Bierbaum V. M., 2009, ApJ, 704, 274
Martín-Doménech R., Öberg K. I., Rajappan M., 2020, IAU Symp , 350, 417
Matar E., Congiu E., Dulieu F., Momeni A., Lemaire J. L., 2008, A&A, 492, L17
McCormac B. M., 1973, Physics and Chemistry of Upper Atmospheres, Astrophysics and Space Science Library, Vol. 35. Reidel Dordrecht
McGuire B. A. et al., 2021, Science, 371, 1265
Miyauchi N., Hidaka H., Chigai T., Nagaoka A., Watanabe N., Kouchi A., 2008, Che. Phys. Lett., 456, 27
Mohamed Ibrahim A. S., Morisset S., Baouche S., Dulieu F., 2022, J. Chem. Phys., 156, 194307
Mokrane H., Chaabouni H., Accola M., Congiu E., Dulieu F., Chehrouri M., Lemaire J. L., 2009, SF2A-2009: Proceedings of the Annual meeting of the French Society of Astronomy and Astrophysics, p. 195
Noble J. A., Jouvet C., Aupetit C., Moudens A., Mascetti J., 2017, A&A, 599, A124
Noble J. A., Michoulier E., Aupetit C., Mascetti J., 2020, A&A, 644, A22
Oba Y., Miyauchi N., Hidaka H., Chigai T., Watanabe N., Kouchi A., 2009, ApJ, 701, 464
Oba Y., Watanabe N., Kouchi A., Hama T., Pirronello V., 2011, PCCP (Incorporating Faraday Trans), 13, 15792
Oba Y., Watanabe N., Hama T., Kuwahata K., Hidaka H., Kouchi A., 2012, ApJ, 749, 67
Oomens J., Sartakov B. G., Tielens A. G. G. M., Meijer G., von Helden G., 2001, ApJ, 560, L99
Papoular R., 2005, MNRAS, 362, 489
Parise, 2004, PhD thesis, CESR (Toulouse, France)
Parise B., Ceccarelli C., Maret S., 2005, A&A, 441, 171
Peeters E., Tielens A. G. G. M., van Kerckhoven C., Hony S., Allamandola L. J., Hudgins D. M., Bauschlicher C. W., 2002, Hot Star Workshop III: The Earliest Stages of Massive Star Birth. ASP Conference Proceedings, 267, 403
Perotti G. et al., 2023, Nature, 620, 516
Potapov A., Jäger C., Henning T., 2019, ApJ, 880, 12
Poteet C. A., Whittet D. C. B., Draine B. T., 2015, ApJ, 801, 110
Puget J. L., Leger A., 1989, ARA&A, 27, 161
Rauls E., Hornekær L., 2008, ApJ, 679, 531
Romanzin C., Ioppolo S., Cuppen H. M., van Dishoeck E. F., Linnartz H., 2011, J. Chem. Phys., 134, 084504
Sadjadi S., Zhang Y., Kwok S., 2015, ApJ, 801, 34
Salama F., 2008, Organic Matter in Space, Proceedings of the International Astronomical Union, IAU Symposium, 251, 357
Silva L., Vladilo G., Murante G., Provenzale A., 2017, MNRAS, 470, 2270
Thrower J. D., Friis E. E., Skov A. L., Jørgensen B., Hornekær L., 2014, PCCP (Incorporating Faraday Trans.), 16, 3381
Tielens A. G. G. M., 2008, ARA&A, 46, 289
Tielens A. G. G. M., Hagen W., 1982, A&A, 114, 245
Tinacci L., Germain A., Pantaleone S., Ceccarelli C., Balucani N., Ugliengo P., 2023, ApJ, 951, 32
van Dishoeck E. F., 2004, ARA&A, 42, 119
van Dishoeck E. F., Herbst E., Neufeld D. A., 2013, Chem. Rev., 113, 9043
Vidali G., Jing D., He J., 2013, AIP Conference Proceedings, 1543, 31
Wakelam V. et al., 2017, Mol. Astrophys., 9, 1
Wang S., Li A., Jiang B. W., 2015, MNRAS, 454, 569
Whittet D. C. B., 2010, ApJ, 710, 1009

This paper has been typeset from a TEX/LATEX file prepared by the author.